Probabilistic Forecasts in Hierarchical Time Series

Abstract

Forecast reconciliation involves adjusting forecasts to ensure coherence with aggregation constraints. We extend this concept from point forecasts to probabilistic forecasts by redefining forecast reconciliation in terms of linear functions in general, and projections more specifically. New theorems establish that the true predictive distribution can be recovered in the elliptical case by linear reconciliation, and general conditions are derived for when this is a projection. A geometric interpretation is also used to prove two new theoretical results for point forecasting; that reconciliation via projection both preserves unbiasedness and dominates unreconciled forecasts in a mean squared error sense. Strategies for forecast evaluation based on scoring rules are discussed, and it is shown that the popular log score is an improper scoring rule with respect to the class of unreconciled forecasts when the true predictive distribution coheres with aggregation constraints. Finally, evidence from a simulation study shows that reconciliation based on an oblique projection, derived from the MinT method of Wickramasuriya et al. (2018) for point forecasting, outperforms both reconciled and unreconciled alternatives.

1 Introduction

Large collections of time series often follow some aggregation structure. For example, the electricity demand of a country can be disaggregated according to a geographic hierarchy of states, cities, and individual households. To ensure aligned decision making, it is important that forecasts at the most disaggregated level add up to forecasts at more aggregated levels. This property is called "coherence". On the other hand "reconciliation" is a process whereby incoherent forecasts are made coherent. Both of these concepts have been developed extensively for point forecasting. Generalising both of these concepts, particularly the latter, to probabilistic forecasting is a gap that we seek to address in this work. We do so by first providing a novel geometric interpretation to coherence and reconciliation in the point forecasting case. This can easily be generalised to probabilistic forecasting allowing us to derive further results for elliptical distributions as well as provide insight into forecast evaluation via multivariate scoring rules.

Traditional approaches to ensure coherent point forecasts produce first-stage forecasts at a single level of the hierarchy. To describe these we use the small hierarchy in Figure 1 where the variable labelled Tot is the sum of the series A and series B, the series A is the sum of series AA and series AB and the series B is the sum of the series BA and BB. In the bottom-up approach (Dunn et al. 1976), forecasts are produced at the most disaggregated level (series AA, AB, BA and BB) and then summed to recover all higher-level series. Alternatively, in the top-down approach (Gross & Sohl 1990), a top-level forecast is first produced (series Tot) and bottom-level forecasts are recovered by disaggregating the forecast using either historical or forecasted proportions. A middle-out approach is a hybrid between these two, that for the hierarchy below would produce first stage forecasts for series A and B.

```
                    Tot
                   /    \
                  A      B
                 / \    / \
               AA  AB  BA  BB
```
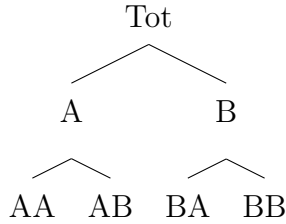
Figure 1: An example of a two level hierarchical structure.

In recent years, reconciliation methods introduced by Hyndman et al. (2011) have become increasingly popular. For these methods, first stage forecasts are independently produced for all series rather than series at a single level. Since these so-called 'base' forecasts are rarely coherent in practice, they are subsequently adjusted or 'reconciled' to ensure coherence. Note that we use coherence and reconciliation as distinct terms, in contrast to their at times ambiguous usage in the past. To date, reconciliation has typically been formulated as a regression problem with alternative reconciliation methods resembling different least squares estimators. These include Ordinary Least Squares OLS (Athanasopoulos et al. 2009), Weighted Least Squares WLS (Athanasopoulos et al. 2017), and a Generalised Least Squares (GLS) estimator (Wickramasuriya et al. 2018) named MinT since it minimises the trace of the squared error matrix. These methods have been shown to outperform traditional alternatives across a range of simulated and real-world datasets (Hyndman et al. 2011, van Erven & Cugliari 2014, Wickramasuriya et al. 2018) since they use information at all levels of the hierarchy and, in some sense, hedge against the risk of model misspecification at a single level.

A shortcoming of the existing literature is a focus on point forecasting despite an increased understanding over the past decade of the importance of providing a full predictive distribution for forecast uncertainty (see Gneiting & Katzfuss 2014, and references therein).

Indeed to the best of our knowledge, the (as yet unpublished) work of (Ben Taieb et al. 2017) is the only paper to deal with coherent probabilistic forecasts, and although they reconcile the means of the predictive distributions, the overall distributions are constructed in a bottom-up fashion rather than use a reconciliation process. In contrast, the main objective of our paper is to generalise both coherence and reconciliation from point to probabilistic forecasting.

To facilitate the extension of point forecast reconciliation to probabilistic forecasting, we first provide a geometric interpretation of existing point reconciliation methods, framing them in terms of projections. In addition to being highly intuitive, this allows us to establish a number of theoretical results. We prove two new theorems about point forecast reconciliation, the first showing that reconciliation via projections preserves the unbiasedness of base forecasts, while the second shows that reconciled forecasts dominate unreconciled forecasts via the distance reducing property of projections. We provide definitions of coherence and forecast reconciliation in the probabilistic setting, and describe how these definitions lead to a reconciliation procedure that merely involves a change of basis and marginalisation. We show that probabilistic reconciliation via linear transformations can recover the true predictive distribution as long as the latter is in the elliptical class. We provide conditions for which this linear transformation is a projection, and although this projection cannot be feasibly estimated in practice, we provide a heuristic argument in favour of MinT reconciliation.

We also cover the topic of forecast evaluation of probabilistic forecasts via scoring rules. In particular, we prove that for a coherent data generating process, the log score is not proper with respect to incoherent forecasts. Therefore we recommend the use of the energy score or variogram score for comparing reconciled to unreconciled forecasts. Two or more reconciled forecasts can be compared using log score, energy score or variogram score,

although we show that comparisons should be made on the full hierarchy for the latter two scores.

The remainder of the paper is structured as follows. In Section 2 coherence is defined geometrically for both point and probabilistic forecasts. Section 3 contains definitions of point and probabilistic forecast reconciliation as well as our main theoretical results. In Section 4 we consider the evaluation of probabilistic hierarchical forecasts via scoring rules, while a simulation study comparing unreconciled probabilistic forecasts and different kinds of reconciled probabilistic forecasts is provided in Section 5. Section 6 concludes with some discussion and thoughts on future research.

2 Coherent forecasts

2.1 Notation and preliminaries

A *hierarchical time series* is a collection of n variables indexed by time, where some variables are aggregates of other variables. We let $\boldsymbol{y}_t \in \mathbb{R}^n$ be a vector comprising observations of all variables in the hierarchy at time t. The *bottom-level series* are defined as those m variables that cannot be formed as aggregates of other variables; we let $\boldsymbol{b}_t \in \mathbb{R}^m$ be a vector comprised of observations of all bottom-level series at time t. The hierarchical structure of the data imply the following holds for all t:

$$\boldsymbol{y}_t = \boldsymbol{S}\boldsymbol{b}_t, \tag{1}$$

where $\boldsymbol{S}$ is an $n \times m$ constant matrix that encodes the aggregation constraints.

To clarify these concepts consider the example of the hierarchy in Figure 1, $n = 7$ and $\boldsymbol{y}_t = [y_{Tot,t}, y_{A,t}, y_{B,t}, y_{C,t}, y_{AA,t}, y_{AB,t}, y_{BA,t}, y_{BB,t}]'$. For example, for the hierarchy in

Figure 1, $m = 4$ and $\boldsymbol{b}_t = [y_{AA,t}, y_{AB,t}, y_{BA,t}, y_{BB,t}]'$. For the hierarchy in Figure 1

$$
\boldsymbol{S} = \begin{pmatrix} 1 & 1 & 1 & 1 \\ 1 & 1 & 0 & 0 \\ 0 & 0 & 1 & 1 \\ & & \boldsymbol{I}_4 & \end{pmatrix},
$$

where $\boldsymbol{I}_4$ is the 4×4 identity matrix.

While most applications of hierarchical time series to date have involved data that respect an aggregation structure, in principle the $\boldsymbol{S}$ can encode any linear constraints including weighted sums or even cases where some variables in the hierarchy are formed by taking the difference of two other variables.

2.2 Coherent point forecasts

It is desirable that forecasts, whether point forecasts or probabilistic forecasts, should in some sense respect the inherent aggregation constraints. We follow other authors (Wickramasuriya et al. 2018, Hyndman & Athanasopoulos 2018) in using the nomenclature *coherence* to describe this property. We now provide new definitions for coherent forecasts in terms of vector spaces that give a geometric understanding of the problem, thus facilitating the development of the probabilistic forecast reconciliation in Section 3.

Definition 2.1 (Coherent subspace). The m-dimensional linear subspace $\mathfrak{s} \subset \mathbb{R}^n$ that is spanned by the columns of $\boldsymbol{S}$, i.e. $\mathfrak{s} = \mathrm{span}(\boldsymbol{S})$, is defined as the *coherent space*.

It will sometimes be useful to think of pre-multiplication by $\boldsymbol{S}$ as a mapping from $\mathbb{R}^m$ to $\mathbb{R}^n$, in which case we use the notation $s(.)$. Although the codomain of $s(.)$ is $\mathbb{R}^n$, its image is the coherent space $\mathfrak{s}$ as depicted in Figure 2.
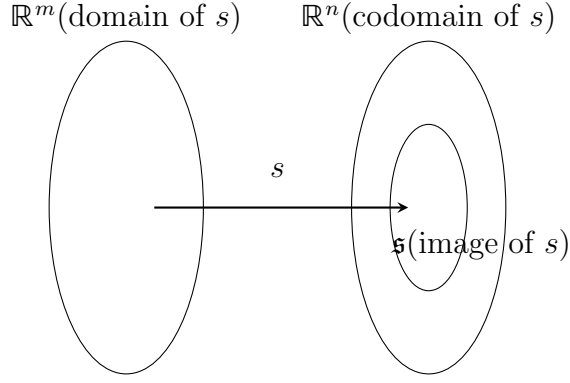
$\mathbb{R}^m$(domain of s) $\mathbb{R}^n$(codomain of s)

s

$\mathfrak{s}$(image of s)

Figure 2: The domain, codomain and image of the mapping s.

Definition 2.2 (Coherent Point Forecasts)**.** Let $\breve{\boldsymbol{y}}_{t+h|t} \in \mathbb{R}^n$ be a point forecast of the values of all series in the hierarchy at time $t+h$, made using information up to and including time t. Then $\breve{\boldsymbol{y}}_{t+h|t}$ is *coherent* if $\breve{\boldsymbol{y}}_{t+h|t} \in \mathfrak{s}$.

2.3 Coherent probabilistic forecasts

Let $(\mathbb{R}^m, \mathscr{F}_{\mathbb{R}^m}, \nu)$ be a probability triple, where $\mathscr{F}_{\mathbb{R}^m}$ is the usual Borel σ-algebra on $\mathbb{R}^m$. Let $\breve{\nu}$ be a probability measure on $\mathfrak{s}$ with σ-algebra $\mathscr{F}_{\mathfrak{s}}$. Here $\mathscr{F}_{\mathfrak{s}}$ is a collection of sets $s(\mathcal{B})$, where $s(\mathcal{B})$ denotes the image of the set $\mathcal{B} \in \mathscr{F}_{\mathbb{R}^m}$ under the mapping $s(.)$.

Definition 2.3 (Coherent Probabilistic Forecasts)**.** The measure $\breve{\nu}$ is coherent if it has the property

$$\breve{\nu}(s(\mathcal{B})) = \nu(\mathcal{B}) \quad \forall \mathcal{B} \in \mathscr{F}_{\mathbb{R}^m},$$

A probabilistic forecast for time $t + h$ is coherent if uncertainty in $\boldsymbol{y}_{t+h}$ conditional on all information up to time t is characterised by the probability triple $(\mathfrak{s}, \mathscr{F}_{\mathfrak{s}}, \breve{\nu})$.

These definitions of the coherent space $\mathfrak{s}$, and coherent point and probabilistic forecasts in terms of the mapping $s(.)$, may give the impression that the bottom-level series play an important role in the definition. However, alternative definitions could be formed using any set of basis vectors that span $\mathfrak{s}$. For example, consider the most simple three variable hierarchy where $y_{1,t} = y_{2,t} + y_{3,t}$. In this case the matrix $\boldsymbol{S}$ has columns $(1,1,0)'$ and $(1,0,1)'$ spanning $\mathfrak{s}$, and pre-multiplying by $\boldsymbol{S}$ transforms arbitrary values of $y_{2,t}$ and $y_{3,t}$ into a coherent vector for the full hierarchy. However the columns $(1,0,1)'$ and $(0,1,-1)'$ also span $\mathfrak{s}$ and define a mapping that transforms arbitrary values of $y_{1,t}$ and $y_{2,t}$ into a coherent vector for the full hierarchy. The definitions above could be made in terms of any series and not just the bottom-level series. In general, we call the series (or linear combinations thereof) used in the definitions of coherence *basis series*. Unless stated otherwise, we will always assume that the basis series are the bottom-level series as in Definition 2.2 and Definition 2.3, since this facilitates comparison with existing approaches in the literature.

To the best of our knowledge, the only other definition of coherent probabilistic forecasts is given by Ben Taieb et al. (2017) who define coherent probabilistic forecasts in terms of convolutions. According to their definition, probabilistic forecasts are coherent when a convolution of forecast distributions of disaggregate series is identical to the forecast distribution of the corresponding aggregate series. Their definition is consistent with our definition; our reason for providing a different definition is that the geometric understanding of coherence will facilitate our definitions of point and probabilistic forecast reconciliation to which we now turn our attention.

8

3 Forecast reconciliation

As discussed, reconciliation is distinct from coherence, since the former refers to a process whereby incoherent forecasts are made coherent. Although reconciliation methods for point forecasts are extant in the literature they are rarely defined explicitly. We do so here in slightly more general terms than usual. We then extend this idea to the novel concept of probabilistic reconciliation.

3.1 Point forecast reconciliation

Let $\hat{\boldsymbol{y}}_{t+h|t} \in \mathbb{R}^n$ be any set of incoherent point forecasts at time $t + h$ conditional on information up to and including time t. We now introduce a linear function that converts unreconciled forecasts into new bottom level forecasts. Let $\boldsymbol{G}$ and $\boldsymbol{d}$ be an $m \times n$ matrix and $m \times 1$ vector respectively, and let $g : \mathbb{R}^n \to \mathbb{R}^m$ be the mapping $g(\boldsymbol{y}) = \boldsymbol{G}\boldsymbol{y} + \boldsymbol{d}$. A composition of g and $s(.)$ gives the following definition for point forecast reconciliation.

Definition 3.1. The point forecast $\tilde{\boldsymbol{y}}_{t+h|t}$ "reconciles" $\hat{\boldsymbol{y}}_{t+h|t}$ with respect to the mapping $g(.)$ iff

$$\tilde{\boldsymbol{y}}_{t+h|t} = \boldsymbol{S}(\boldsymbol{G}\hat{\boldsymbol{y}}_{t+h|t} + \boldsymbol{d}) . \tag{2}$$

Several choices of $g(.)$ currently extant in the literature, including the OLS, WLS and MinT methods, are special cases where $s \circ g$ is a projection. These can be defined so that $\boldsymbol{G} = (\boldsymbol{R}'_\perp \boldsymbol{S})^{-1} \boldsymbol{R}'_\perp$ and $\boldsymbol{d} = \boldsymbol{0}$, were, $\boldsymbol{R}_\perp$ is a $n \times m$ orthogonal complement to an $n \times (n - m)$ matrix $\boldsymbol{R}$, where the columns of the latter span the null space of $\mathfrak{s}$. For example, a straightforward choice of $\boldsymbol{R}$ for the most simple three variable hierarchy where $y_{1,t} = y_{2,t} + y_{3,t}$, is the vector $(1, -1, -1)$ which is orthogonal (in the Euclidean sense) to the columns of $\boldsymbol{S}$. In this case, the matrix $\boldsymbol{R}$ can be interpreted as a 'restrictions' matrix

since it has the property that $\boldsymbol{R}'\boldsymbol{y} = \boldsymbol{0}$ for coherent $\boldsymbol{y}$. For this three variable hierarchy, $\boldsymbol{R}'_\perp = \boldsymbol{S}$ and reconciliation corresponds to the OLS method. For the case where $\boldsymbol{R}'_\perp \neq \boldsymbol{S}$, for example WLS and MinT, there are two possible interpretations. One is that these are oblique projections in Euclidean space where the columns of $\boldsymbol{R}$ are 'directions' along which incoherent point forecasts are projected onto the coherent space $\mathfrak{s}$. Alternatively, since $\boldsymbol{R}'_\perp$ is usually written in the form $\boldsymbol{S}'\boldsymbol{W}^{-1}$, these projections can be thought of as orthogonal projections after pre-multiplying by $\boldsymbol{W}^{-1/2}$. A schematic providing a geometric interpretation of point reconciliation is given in Figure 3, while Table 1 summarises existing reconciliation methods.

Table 1: Summary of reconciliation methods that are projections. Here, $\hat{\boldsymbol{W}}^{sam}$ is the variance covariance matrix of one-step ahead forecast errors, $\hat{\boldsymbol{W}}^{shr}$ is a shrinkage estimator more suited to large dimensions proposed by Schäfer & Strimmer (2005), $\hat{\boldsymbol{W}}^{wls}$ is the diagonal matrix with diagonal elements w_{ii}, and $\tau = \frac{\sum_{i \neq j} \hat{\mathrm{Var}}(\hat{w}_{ij})}{\sum_{i \neq j} \hat{w}_{ij}^2}$, where w_{ij} denotes the (i,j)th element of $\hat{\boldsymbol{W}}^{sam}$.

Method	$\boldsymbol{W}$	$\boldsymbol{R}'_\perp$
OLS	$\boldsymbol{I}$	$\boldsymbol{S}'$
MinT(Sample)	$\hat{\boldsymbol{W}}^{sam}$	$\boldsymbol{S}'(\hat{\boldsymbol{W}}^{sam})^{-1}$
MinT(Shrink)	$\tau\mathrm{Diag}(\hat{\boldsymbol{W}}^{sam}) + (1-\tau)\hat{\boldsymbol{W}}^{sam}$	$\boldsymbol{S}'(\hat{\boldsymbol{W}}^{shr})^{-1}$
WLS	$\mathrm{Diag}(\hat{\boldsymbol{W}}^{shr})$	$\boldsymbol{S}'(\hat{\boldsymbol{W}}^{wls})^{-1}$

The columns of $\boldsymbol{S}$ and $\boldsymbol{R}$ provide a basis for $\mathbb{R}^n$. Therefore any incoherent set of point forecasts $\hat{\boldsymbol{y}}_{t+h|t} \in \mathbb{R}^n$ can be expressed in terms of coordinates in the basis defined by $\boldsymbol{S}$ and $\boldsymbol{R}$. Let $\tilde{\boldsymbol{b}}_{t+h|t}$ and $\tilde{\boldsymbol{a}}_{t+h|t}$ be the coordinates corresponding to $\boldsymbol{S}$ and $\boldsymbol{R}$ respectively, after a change of basis. The process of reconciliation involves setting the values of the reconciled
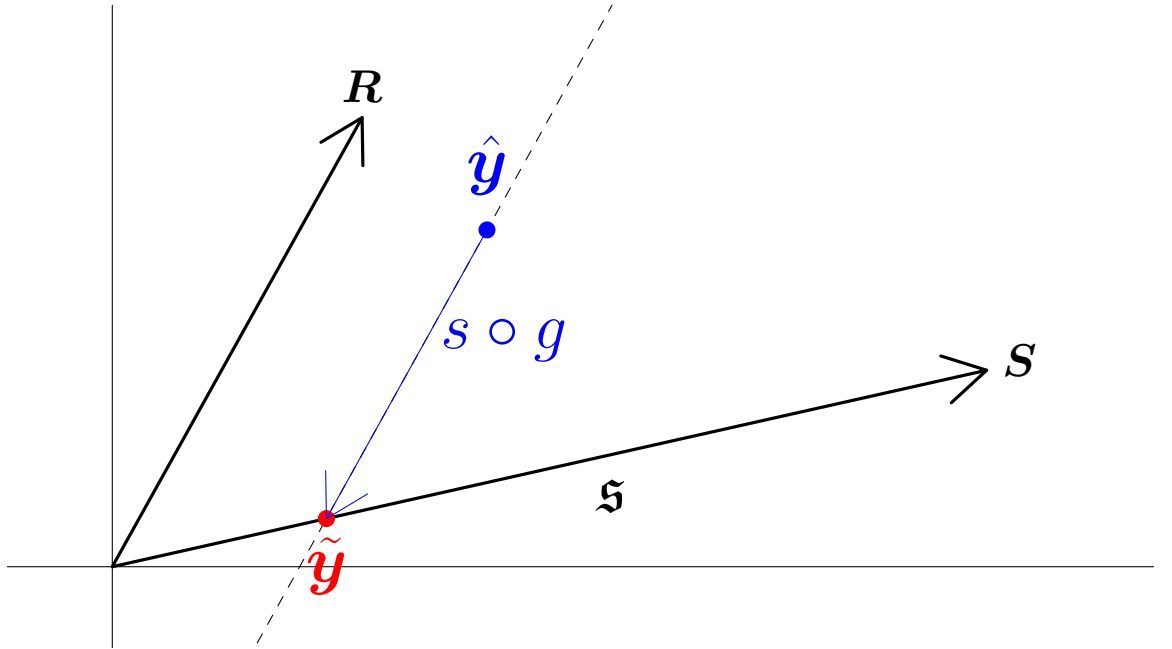
Figure 3: Summary of probabilistic point reconciliation. The mapping $s \circ g$ projects the unreconciled forecast $\hat{\boldsymbol{y}}$ onto $\mathfrak{s}$. Since the smallest hierarchy involves three dimensions, this figure is only a schematic.

bottom-level series to be $\tilde{\boldsymbol{b}}_{t+h|t}$, and ignoring $\tilde{\boldsymbol{a}}_{t+h}$ to ensure coherence. From properties of linear algebra it follows that

$$\hat{\boldsymbol{y}}_{t+h|t} = (\boldsymbol{S}\ \boldsymbol{R}) \begin{pmatrix} \tilde{\boldsymbol{b}}_{t+h|t} \\ \tilde{\boldsymbol{a}}_{t+h|t} \end{pmatrix} = \boldsymbol{S}\tilde{\boldsymbol{b}}_{t+h|t} + \boldsymbol{R}\tilde{\boldsymbol{a}}_{t+h|t},$$

while the reconciled point forecast is

$$\tilde{\boldsymbol{y}}_{t+h|t} = \boldsymbol{S}\tilde{\boldsymbol{b}}_{t+h|t}.$$

In order to find $\tilde{\boldsymbol{b}}_{t+h|t}$ we require the inverse $(\boldsymbol{S}\ \boldsymbol{R})^{-1}$ which is given by

$$(\boldsymbol{S}\ \boldsymbol{R})^{-1} = \begin{pmatrix} (\boldsymbol{R}'_\perp \boldsymbol{S})^{-1}\boldsymbol{R}'_\perp \\ (\boldsymbol{S}'_\perp \boldsymbol{R})^{-1}\boldsymbol{S}'_\perp \end{pmatrix}, \tag{3}$$

where $\boldsymbol{S}_\perp$ is the orthogonal complements of $\boldsymbol{S}$. Thus it follows that $\tilde{\boldsymbol{b}}_{t+h} = (\boldsymbol{R}'_\perp \boldsymbol{S})^{-1}\boldsymbol{R}'_\perp \hat{\boldsymbol{y}}_{t+h}$ and $\tilde{\boldsymbol{y}}_{t+h|t} = \boldsymbol{S}(\boldsymbol{R}'_\perp \boldsymbol{S})^{-1}\boldsymbol{R}'_\perp \hat{\boldsymbol{y}}_{t+h|t}$. Here $(\boldsymbol{R}'_\perp \boldsymbol{S})^{-1}\boldsymbol{R}'_\perp$ corresponds to $\boldsymbol{G}$ as defined previously.

Point reconciliation methods based on projections will always minimise the distance between unreconciled and reconciled forecasts, however the specific distance will depend on the choice of $\boldsymbol{R}$. For example OLS minimises the Euclidean distance between $\hat{\boldsymbol{y}}$ and $\tilde{\boldsymbol{y}}$, while Wickramasuriya et al. (2018) show that MinT minimises the Mahalonobis distance between $\hat{\boldsymbol{y}}$ and $\tilde{\boldsymbol{y}}$. Bottom-up methods minimise distance between reconciled and unreconciled forecasts only along dimensions corresponding to the bottom-level series. Therefore bottom-up methods should be thought of as a boundary case of reconciliation methods, since they ultimately do not use information at all levels of the hierarchy.

Before generalising the concept of point reconciliation to probabilistic forecasts, we state two theorems that motivate the use of projections for point forecast reconciliation. First, let $\boldsymbol{\mu}_{t+h|t} := \mathrm{E}(\boldsymbol{y}_{t+h} \mid \boldsymbol{y}_1, \ldots, \boldsymbol{y}_t)$ and assume $\hat{\boldsymbol{y}}_{t+h|t}$ is an unbiased prediction; that

12

is $\mathrm{E}_{1:t}(\hat{\boldsymbol{y}}_{t+h|t}) = \mu_{t+h|t}$, where the subscript $1:t$ denotes an expectation taken over the training sample.

Theorem 3.1 (Unbiasedness preserving property)**.** *For unbiased $\hat{\boldsymbol{y}}_{t+h|t}$, the reconciled point forecast is also be an unbiased prediction as long as $s \circ g$ is a projection.*

Proof. The expected value of the reconciled forecast is given by

$$\mathrm{E}_{1:t}(\tilde{\boldsymbol{y}}_{t+h|t}) = \mathrm{E}_{1:t}(\boldsymbol{SG}\hat{\boldsymbol{y}}_{t+h|t}) = \boldsymbol{SG}\mathrm{E}_{1:t}(\hat{\boldsymbol{y}}_{t+h|t}) = \boldsymbol{SG}\boldsymbol{\mu}_{t+h|t}.$$

Since the aggregation constraints hold for the true data generating process, $\boldsymbol{\mu}_{t+h|t}$ must lie in $\mathfrak{s}$. If $\boldsymbol{SG}$ is a projection, then it is equivalent to the identity map for all vectors that lie in its range. Therefore $\boldsymbol{SG}\boldsymbol{\mu}_{t+h|t} = \boldsymbol{\mu}_{t+h|t}$ when $\boldsymbol{SG}$ is a projection matrix. $\qquad\square$

We note the same result does not hold for general g even when the range of $s \circ g$ is $\mathfrak{s}$. Now let $\boldsymbol{y}_{t+h}$ be the realisation of the data generating process at time $t+h$, and let $\|\boldsymbol{v}\|_2$ be the L_2 norm of vector $\boldsymbol{v}$. The following theorem shows that reconciliation never increases, and in most cases reduces, the sum of squared errors of point forecasts.

Theorem 3.2 (Distance reducing property)**.** *If $\tilde{\boldsymbol{y}}_{t+h|t} = \boldsymbol{SG}\hat{\boldsymbol{y}}_{t+h|t}$, where $\boldsymbol{G}$ is such that $\boldsymbol{SG}$ is an orthogonal projection onto $\mathfrak{s}$, then the following inequality holds:*

$$\|(\tilde{\boldsymbol{y}}_{t+h|t} - \boldsymbol{y}_{t+h})\|_2^2 \leq \|(\hat{\boldsymbol{y}}_{t+h|t} - \boldsymbol{y}_{t+h})\|_2^2. \tag{4}$$

Proof. Since the aggregation constraints must hold for all realisations, $\boldsymbol{y}_{t+h} \in \mathfrak{s}$ and $\boldsymbol{y}_{t+h} = \boldsymbol{SG}\boldsymbol{y}_{t+h}$ whenever $\boldsymbol{SG}$ is a projection. Therefore

$$\|(\tilde{\boldsymbol{y}}_{t+h|t} - \boldsymbol{y}_{t+h})\|_2 = \|(\boldsymbol{SG}\hat{\boldsymbol{y}}_{t+h|t} - \boldsymbol{SG}\boldsymbol{y}_{t+h})\|_2 \tag{5}$$

$$= \|\boldsymbol{SG}(\hat{\boldsymbol{y}}_{t+h|t} - \boldsymbol{y}_{t+h})\|_2 \tag{6}$$

$$\tag{7}$$

13

The Cauchy-Schwarz inequality can be used to show that orthogonal projections are bounded operators (Hunter & Nachtergaele 2001), therefore

$$\|\boldsymbol{SG}(\hat{\boldsymbol{y}}_{t+h|t} - \boldsymbol{y}_{t+h})\|_2 \leq \|(\hat{\boldsymbol{y}}_{t+h|t} - \boldsymbol{y}_{t+h})\|_2.$$

□

The inequality is strict whenever $\hat{\boldsymbol{y}}_{t+h|t} \notin \mathfrak{s}$.

3.2 Probabilistic forecast reconciliation

We now extend the methodology of point forecast reconciliation to probabilistic forecasts. Let $(\mathbb{R}^n, \mathscr{F}_{\mathbb{R}^n}, \hat{\nu})$ be a probability triple that is not coherent and which characterises forecast uncertainty for all variables in the hierarchy at time $t+h$ conditional on all information up to time t. This is obtained from the first stage of the forecasting process; e.g., by modelling and forecasting each series individually. Let $g : \mathbb{R}^n \to \mathbb{R}^m$ be a linear function, and let $(\mathbb{R}^m, \mathscr{F}_{\mathbb{R}^m}, \nu)$ be a probability triple defined on $\mathbb{R}^m$.

Definition 3.2. The reconciled probability measure of $\hat{\nu}$ with respect to the mapping $g(.)$ is a probability measure $\tilde{\nu}$ on $\mathfrak{s}$ with σ-algebra $\mathscr{F}_{\mathfrak{s}}$ such that

$$\tilde{\nu}(s(\mathcal{B})) = \nu(\mathcal{B}) = \hat{\nu}(g^{-1}(\mathcal{B})) \qquad \forall \mathcal{B} \in \mathscr{F}_{\mathbb{R}^m} , \tag{8}$$

where $g^{-1}(\mathcal{B}) := \{\breve{\boldsymbol{y}} \in \mathbb{R}^n : g(\breve{\boldsymbol{y}}) \in \mathcal{B}\}$ is the pre-image of $\mathcal{B}$, that is the set of all points in $\mathbb{R}^n$ that $g(.)$ maps to a point in $\mathcal{B}$.

This definition extends the notion of forecast reconciliation to the probabilistic setting. Under point reconciliation methods, the reconciled point forecast is equal to the unreconciled point forecast after the latter is passed through two linear functions. Similarly, probabilistic forecast reconciliation assigns the same probability to two sets where

14

the points in one set are obtained by passing all points in the other set through two linear functions. This is depicted in Figure 4 schematically when $s \circ g$ is a projection.

Recall that when $s \circ g$ is a projection, the case of point forecast reconciliation can be broken down into three steps.

1. $\hat{\boldsymbol{y}}_{t+h|t}$ is transformed into coordinates $\tilde{\boldsymbol{b}}_{t+h|t}$ and $\tilde{\boldsymbol{a}}_{t+h|t}$ via a change of basis.

2. $\tilde{\boldsymbol{a}}_{t+h|t}$ is discarded and $\tilde{\boldsymbol{b}}_{t+h|t}$ are kept as the bottom-level reconciled forecasts.

3. Reconciled forecasts for the entire hierarchy are recovered via $\tilde{\boldsymbol{y}}_{t+h|t} = \boldsymbol{S}\tilde{\boldsymbol{b}}_{t+h|t}$.

We now outline the analogues to these three steps for probabilistic forecasts when predictive densities are available.

While $\hat{\nu}$ is a probability measure for an n-vector $\hat{\boldsymbol{y}}_{t+h|t}$, probability statements in terms of a different coordinate system can be made via an appropriate change of basis. Letting $f(.)$ be generic notation for a probability density function, and following the notation from our definition of point forecast reconciliation where $\hat{\boldsymbol{y}}_{t+h|t} = \boldsymbol{S}\tilde{\boldsymbol{b}}_{t+h|t} + \boldsymbol{R}\tilde{\boldsymbol{a}}_{t+h|t}$, we obtain

$$f(\hat{\boldsymbol{y}}_{t+h|t}) = f(\boldsymbol{S}\tilde{\boldsymbol{b}}_{t+h|t} + \boldsymbol{R}\tilde{\boldsymbol{a}}_{t+h|t})|(\boldsymbol{S} \ \boldsymbol{R})| \tag{9}$$

The expression $\hat{\nu}(g^{-1}(\mathcal{B}))$ in Definition 3.2 is equivalent to the probability statement $\Pr(\hat{\boldsymbol{y}}_{t+h|t} \in g^{-1}(\mathcal{B}))$. After the change of basis, this is equivalent to $\Pr(\tilde{\boldsymbol{b}} \in \mathcal{B})$, which implies

$$\Pr(\hat{\boldsymbol{y}}_{t+h|t} \in g^{-1}(\mathcal{B})) = \int_{g^{-1}(\mathcal{B})} f(\hat{\boldsymbol{y}}_{t+h|t})d\hat{\boldsymbol{y}}_{t+h|t} \tag{10}$$

$$= \int_{\mathcal{B}} \int f(\boldsymbol{S}\tilde{\boldsymbol{b}}_{t+h|t} + \boldsymbol{R}\tilde{\boldsymbol{a}}_{t+h|t})|(\boldsymbol{S} \ \boldsymbol{R})|d\tilde{\boldsymbol{a}}_{t+h|t}d\tilde{\boldsymbol{b}}_{t+h|t}. \tag{11}$$

After integrating out over $\tilde{\boldsymbol{a}}_{t+h|t}$, a step analogous to setting $\tilde{\boldsymbol{a}}_{t+h|t} = 0$ for point forecasting, we obtain an expression that gives the probability that the reconciled bottom-level series lies in the region $\mathcal{B}$. This corresponds to $\nu(\mathcal{B})$ in Definition 3.2. To make a valid probability
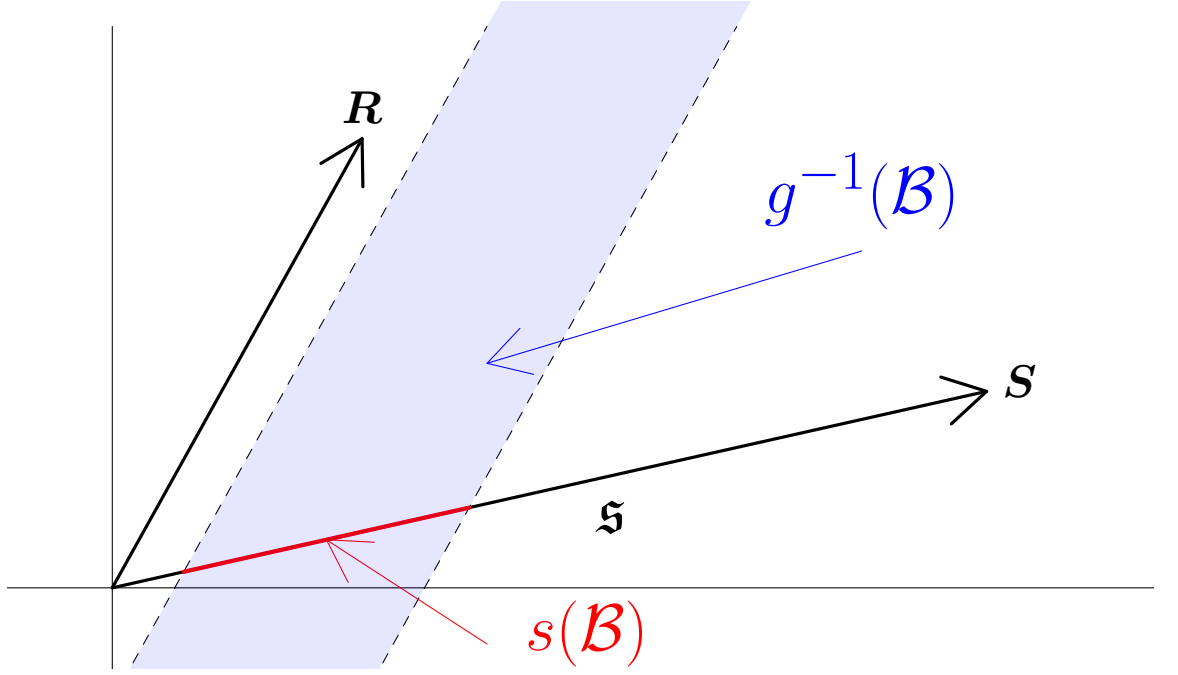
Figure 4: Summary of probabilistic forecast reconciliation. The probability that $\boldsymbol{y}_{t+h}$ lies in the red line segment under the reconciled probabilistic forecast is defined to be equal to the probability that $\boldsymbol{y}_{t+h}$ lies in the shaded blue area under the unreconciled probabilistic forecast. Note that since the smallest hierarchy involves three dimensions, this figure is only a schematic.

statement about the entire hierarchy we simply use the bottom-level probabilistic forecasts together with Definition 2.3.

Example: Gaussian Distributions

Suppose an unreconciled probabilistic forecast is Gaussian with mean $\hat{\boldsymbol{\mu}}$ and variance-covariance matrix $\hat{\boldsymbol{\Sigma}}$. The subscripts $t+h|t$ are suppressed for brevity. The unreconciled density

$$f(\hat{\boldsymbol{y}}) = (2\pi)^{-n/2} |\hat{\boldsymbol{\Sigma}}|^{-1/2} \exp\left\{ -\frac{1}{2} \left[(\hat{\boldsymbol{y}} - \hat{\boldsymbol{\mu}})' \hat{\boldsymbol{\Sigma}}^{-1} (\hat{\boldsymbol{y}} - \hat{\boldsymbol{\mu}}) \right] \right\}. \tag{12}$$

In an alternative basis,

$$f(\tilde{\boldsymbol{b}}, \tilde{\boldsymbol{a}}) = (2\pi)^{-\frac{n}{2}} \left| \hat{\boldsymbol{\Sigma}} \right|^{-\frac{1}{2}} \left| (\boldsymbol{S} \ \boldsymbol{R}) \right| \exp\{ -\frac{1}{2} q \}, \tag{13}$$

where

$$q = (\boldsymbol{S}\tilde{\boldsymbol{b}} + \boldsymbol{R}\tilde{\boldsymbol{a}} - \hat{\boldsymbol{\mu}})' \hat{\boldsymbol{\Sigma}}^{-1} (\boldsymbol{S}\tilde{\boldsymbol{b}} + \boldsymbol{R}\tilde{\boldsymbol{a}} - \hat{\boldsymbol{\mu}}). \tag{14}$$

The quadratic form q can be rearranged as

$$q = \left((\boldsymbol{S} \ \boldsymbol{R}) \begin{pmatrix} \tilde{\boldsymbol{b}} \\ \tilde{\boldsymbol{a}} \end{pmatrix} - \hat{\boldsymbol{\mu}} \right)' \hat{\boldsymbol{\Sigma}}^{-1} \left((\boldsymbol{S} \ \boldsymbol{R}) \begin{pmatrix} \tilde{\boldsymbol{b}} \\ \tilde{\boldsymbol{a}} \end{pmatrix} - \hat{\boldsymbol{\mu}} \right),$$

$$= \left(\begin{pmatrix} \tilde{\boldsymbol{b}} \\ \tilde{\boldsymbol{a}} \end{pmatrix} - (\boldsymbol{S} \ \boldsymbol{R})^{-1} \hat{\boldsymbol{\mu}}_{t+h} \right)' \left[(\boldsymbol{S}\boldsymbol{R})^{-1} \hat{\boldsymbol{\Sigma}}_{t+h} \left((\boldsymbol{S} \ \boldsymbol{R})^{-1} \right)' \right]^{-1} \left(\begin{pmatrix} \tilde{\boldsymbol{b}} \\ \tilde{\boldsymbol{a}} \end{pmatrix} - (\boldsymbol{S} \ \boldsymbol{R})^{-1} \hat{\boldsymbol{\mu}}_{t+h} \right).$$

Recall that

$$(\boldsymbol{S} \ \boldsymbol{R})^{-1} = \begin{pmatrix} (\boldsymbol{R}_\perp' \boldsymbol{S})^{-1} \boldsymbol{R}_\perp' \\ (\boldsymbol{S}_\perp' \boldsymbol{R})^{-1} \boldsymbol{S}_\perp' \end{pmatrix} := \begin{pmatrix} \boldsymbol{G} \\ \boldsymbol{H} \end{pmatrix}.$$

Then q can be rearranged further as

$$q = \left[\begin{pmatrix} \tilde{b} \\ \tilde{a} \end{pmatrix} - \begin{pmatrix} G \\ H \end{pmatrix} \hat{\mu}_{t+h} \right]' \left[\begin{pmatrix} G \\ H \end{pmatrix} \hat{\Sigma}_{t+h} \begin{pmatrix} G \\ H \end{pmatrix}' \right]^{-1} \left[\begin{pmatrix} \tilde{b} \\ \tilde{a} \end{pmatrix} - \begin{pmatrix} G \\ H \end{pmatrix} \hat{\mu}_{t+h} \right]$$

$$= \begin{pmatrix} \tilde{b} - G\hat{\mu} \\ \tilde{a} - H\hat{\mu} \end{pmatrix}' \left[\begin{pmatrix} G \\ H \end{pmatrix} \hat{\Sigma}_{t+h} \begin{pmatrix} G \\ H \end{pmatrix}' \right]^{-1} \begin{pmatrix} \tilde{b} - G\hat{\mu} \\ \tilde{a} - H\hat{\mu} \end{pmatrix}.$$

Similar manipulations on the determinant of the covariance matrix lead to the following expression for the density:

$$f(\tilde{b}, \tilde{a}) = (2\pi)^{-\frac{n}{2}} \left| \begin{pmatrix} G\hat{\Sigma}G' & G\hat{\Sigma}H' \\ H\hat{\Sigma}G' & H\hat{\Sigma}H' \end{pmatrix} \right|^{-\frac{1}{2}} \exp\left\{ -\frac{1}{2} \begin{pmatrix} \tilde{b} - G\hat{\mu} \\ \tilde{a} - H\hat{\mu} \end{pmatrix}' \right.$$
$$\left. \begin{pmatrix} G\hat{\Sigma}G' & G\hat{\Sigma}H' \\ H\hat{\Sigma}G' & H\hat{\Sigma}H' \end{pmatrix}^{-1} \begin{pmatrix} \tilde{b} - G\hat{\mu} \\ \tilde{a} - H\hat{\mu} \end{pmatrix} \right\}.$$

Marginalising out $\tilde{a}$ leads to the following bottom-level reconciled forecasts:

$$f(\tilde{b}) = (2\pi)^{-\frac{m}{2}} \left| G\hat{\Sigma}G' \right|^{\frac{1}{2}} \exp\left\{ -\frac{1}{2}(\tilde{b} - G\hat{\mu})'(G\hat{\Sigma}G')^{-1}(\tilde{b} - G\hat{\mu}) \right\}. \tag{15}$$

This implies that the reconciled probabilistic forecast for the bottom-level series is $\tilde{b}_{t+h} \sim \mathcal{N}(G\hat{\mu}_{t+h}, G\hat{\Sigma}_{t+h}G')$. The reconciled probabilistic forecasts for the whole hierarchy follow a degenerate Gaussian distribution with mean $SG\hat{\mu}$ and rank deficient covariance matrix $SG\hat{\Sigma}_{t+h}G'S'$.

3.3 Elliptical distributions

We now show that the true predictive distribution can be recovered for elliptical distributions by linear reconciliation via pre-multiplication and translation respectively by a matrix

18

we denote $\boldsymbol{G}_{opt}$ and vector we denote $\boldsymbol{d}_{opt}$. Here, for any square matrix $\boldsymbol{C}$, $\boldsymbol{C}^{1/2}$ and $\boldsymbol{C}^{-1/2}$ are defined to satisfy $\boldsymbol{C}^{1/2}(\boldsymbol{C}^{1/2})' = \boldsymbol{C}$ and $\boldsymbol{C}^{-1/2}(\boldsymbol{C}^{-1/2})' = \boldsymbol{C}^{-1}$, for example $\boldsymbol{C}^{1/2}$ may be obtained via the Cholesky or eigenvalue decompositions.

Theorem 3.3 (Reconciliation for Elliptical Distributions). *Let an unreconciled probabilistic forecast come from the elliptical class with location parameter $\hat{\boldsymbol{\mu}}$ and scale matrix $\hat{\boldsymbol{\Sigma}}$. Let the true predictive distribution of $\boldsymbol{y}_{t+h|t}$ also belong to the elliptical class with location parameter $\boldsymbol{\mu}$ and scale matrix $\boldsymbol{\Sigma}$. Then the linear reconciliation mapping $g(\breve{\boldsymbol{y}}) = \boldsymbol{G}_{opt}\breve{\boldsymbol{y}} + \boldsymbol{d}_{opt}$ with $\boldsymbol{G}_{opt} = \boldsymbol{a}\boldsymbol{\Sigma}^{-1/2}$ and $\boldsymbol{d}_{opt} = \boldsymbol{\mu} - \boldsymbol{S}\boldsymbol{G}_{opt}\hat{\boldsymbol{\mu}}$ recovers the true predictive density where $\boldsymbol{a}$ is any $m \times n$ matrix such that $\boldsymbol{a}\boldsymbol{a}' = \boldsymbol{\Omega}$ and $\boldsymbol{\Omega}$ is a sub-matrix of $\boldsymbol{\Sigma}$ corresponding to the bottom-level series.*

Proof. Since elliptical distributions are closed under affine transformations, and are closed under marginalisation, reconciliation of an elliptical distribution yields an elliptical distribution (although the unreconciled and reconciled distributions may be different members of the class of elliptical distributions). The scale matrix of the reconciled forecast is given by $\boldsymbol{S}\boldsymbol{G}_{opt}\boldsymbol{\Sigma}\boldsymbol{G}'_{opt}\boldsymbol{S}'$, while the location matrix is given by $\boldsymbol{S}\boldsymbol{G}_{opt}\hat{\boldsymbol{\mu}} + \boldsymbol{d}_{opt}$. The reconciled scale matrix is

$$\tilde{\boldsymbol{\Sigma}}_{opt} = \boldsymbol{S}\boldsymbol{a}\boldsymbol{\Sigma}^{-1/2}\boldsymbol{\Sigma}\left(\boldsymbol{\Sigma}^{-1/2}\right)'\boldsymbol{a}'\boldsymbol{S}' = \boldsymbol{S}\boldsymbol{\Omega}\boldsymbol{S}' = \boldsymbol{\Sigma}.$$

For the choices of $\boldsymbol{G}_{opt}$ and $\boldsymbol{d}_{opt}$ given above, the reconciled location vector is

$$\tilde{\boldsymbol{\mu}}_{opt} = \boldsymbol{S}\boldsymbol{G}_{opt}\hat{\boldsymbol{\mu}} + \boldsymbol{\mu} - \boldsymbol{S}\boldsymbol{G}_{opt}\hat{\boldsymbol{\mu}} = \boldsymbol{\mu}.$$

$\square$

A number of insights can be drawn from this theorem. First, although a linear function $g(.)$ can be used to recover the true predictive in the elliptical case, the same does not hold

in general. Second, $g(.)$ is not, in general, a projection matrix. The conditions for which a the true predictive density can be recovered by a projection are given below.

Theorem 3.4 (True predictive via projection)**.** *Assume that the true predictive distribution is elliptical with location $\boldsymbol{\mu}$ and scale $\boldsymbol{\Sigma}$. Consider reconciliation via a projection $g(\boldsymbol{y}) = (\boldsymbol{R}'_\perp \boldsymbol{S})^{-1} \boldsymbol{R}'_\perp \boldsymbol{y}$. The true predictive distribution can be recovered via reconciliation of an elliptical distribution with location $\hat{\boldsymbol{\mu}}$ and scale $\hat{\boldsymbol{\Sigma}}$ when the following conditions hold:*

$$sp(\hat{\boldsymbol{\mu}} - \boldsymbol{\mu}) \subset sp(\boldsymbol{R}) \tag{16}$$

$$sp(\hat{\boldsymbol{\Sigma}}^{1/2} - \boldsymbol{\Sigma}^{1/2}) \subset sp(\boldsymbol{R}) \tag{17}$$

$$\tag{18}$$

Proof. The reconciled location vector will be given by

$$\tilde{\boldsymbol{\mu}} = \boldsymbol{S}(\boldsymbol{R}'_\perp \boldsymbol{S})^{-1} \boldsymbol{R}'_\perp \hat{\boldsymbol{\mu}}$$
$$= \boldsymbol{S}(\boldsymbol{R}'_\perp \boldsymbol{S})^{-1} \boldsymbol{R}'_\perp (\hat{\boldsymbol{\mu}} + \boldsymbol{\mu} - \boldsymbol{\mu})$$
$$= \boldsymbol{S}(\boldsymbol{R}'_\perp \boldsymbol{S})^{-1} \boldsymbol{R}'_\perp \boldsymbol{\mu} + \boldsymbol{S}(\boldsymbol{R}'_\perp \boldsymbol{S})^{-1} \boldsymbol{R}'_\perp (\hat{\boldsymbol{\mu}} - \boldsymbol{\mu}).$$

Since $\boldsymbol{S}(\boldsymbol{R}'_\perp \boldsymbol{S})^{-1} \boldsymbol{R}'_\perp$ is a projection onto $\mathfrak{s}$ and $\boldsymbol{\mu} \in \mathfrak{s}$, the first term simplifies to $\boldsymbol{\mu}$. If $\boldsymbol{\mu} - \hat{\boldsymbol{\mu}}$ lies in the span of $\boldsymbol{R}$, then multiplication by $\boldsymbol{R}'_\perp$ reduces the second term to $\boldsymbol{0}$. By a similar argument it can be shown that $\tilde{\boldsymbol{\Sigma}}^{1/2} = \boldsymbol{\Sigma}^{1/2}$. The closure property of elliptical distributions under affine transformations ensures that the full true predictive distribution can be recovered. $\qquad\square$

Although these conditions will rarely hold in practice and only apply to a limited class of distributions, they do provide some insight into selecting a projection for reconciliation. If the value of $\hat{\boldsymbol{\mu}}$ were equi-probable in all directions, then a projection orthogonal to $\mathfrak{s}$ would be a sensible choice for $\boldsymbol{R}$ since it would in some sense represent a 'median' direction for

$\boldsymbol{\mu} - \hat{\boldsymbol{\mu}}$. However, the one-step-ahead in-sample errors are usually correlated suggesting that $\hat{\boldsymbol{\mu}}$ is more likely to fall in some directions than others. Therefore an orthogonal projection after transformation by the inverse of the one-step-ahead in-sample error covariance matrix may be more intuitively appealing. This is exactly what the MinT projection provides, and as simulations will show in Section 5, this projection leads to the best empirical results.

4 Evaluation of hierarchical probabilistic forecasts

The necessary final step in hierarchical forecasting is to make sure that our forecast distributions are accurate. In general, forecasters prefer to maximize the sharpness of the forecast distribution subject to calibration (Gneiting & Katzfuss 2014). Therefore the probabilistic forecasts should be evaluated with respect to these two properties.

Calibration refers to the statistical compatibility between probabilistic forecasts and realizations. In other words, random draws from a perfectly calibrated forecast distribution should be equivalent in distribution to the realizations. On the other hand, sharpness refers to the spread or the concentration of the predictive distributions and it is a property of the forecasts only. The more concentrated the forecast distributions, the sharper the forecasts (Gneiting et al. 2008). However, independently assessing the calibration and sharpness will not help to properly evaluate the probabilistic forecasts. Therefore we need to assess these properties simultaneously using scoring rules.

Scoring rules are summary measures obtained based on the relationship between the forecast distributions and the realizations. In some studies, researchers take the scoring rules to be positively oriented, in which case the scores should be maximized (Gneiting & Raftery 2007). However, scoring rules have also been defined to be negatively oriented, and then the scores should be minimized (Gneiting & Katzfuss 2014). We follow the latter

convention here.

Let P be a forecast distribution and let Q be the true data generating process respectively. Furthermore let ω be a realization from Q. Then a scoring rule is a function $S(P,\omega)$ that maps P,ω to $\mathbb{R}$. It is a "proper" scoring rule if

$$\mathrm{E}_{\boldsymbol{Q}}[S(Q,\omega)] \leq \mathrm{E}_{\boldsymbol{Q}}[S(P,\omega)], \tag{19}$$

where $\mathrm{E}_Q[S(P,\omega)]$ is the expected score under the true distribution Q (Gneiting et al. 2008, Gneiting & Katzfuss 2014). When this inequality is strict, the scoring rule is said to be strictly proper.

In the context of probabilistic forecast reconciliation there could be two motivations for using scoring rules. The first is to compare unreconciled densities to reconciled densities. Reconciliation itself is a valuable goal since it can be important in aligning decision making across, for example, different units of an enterprise. In the point forecasting literature, forecast reconciliation has also been shown to improve forecast performance (Athanasopoulos et al. 2017, Wickramasuriya et al. 2018). It will be worthwhile to see whether the same holds in the probabilistic forecasting case. The second motivation for using scoring rules is to compare two or more sets of reconciled probabilistic forecasts to one another. The objective here is to evaluate which reconciliation mapping $g(.)$ works best in practice.

4.1 Univariate scoring rules

One way to evaluate hierarchical probabilistic forecasts is via the application of univariate scoring rules to each variable in the hierarchy. A summary can be taken of the expected scores across each margin, for example a mean or median. In the simulations of Section 5, we consider two scoring rules. The log score is given by the log density, in this case for each margin of the probabilistic forecast. The cumulative rank probability score generalises

mean square error and is given by

$$\text{CRPS}(\breve{F}_i, y_i) = \int \left(\breve{F}_i(\breve{Y}_i) - \mathbb{1}\left(y_i < y_i\right) \right) d\breve{Y}_i \tag{20}$$

$$= \mathrm{E}_{\breve{Y}_i}|\breve{Y}_i - y_i| - \frac{1}{2}\mathrm{E}_{\breve{Y}_i}|\breve{Y}_i - \breve{Y}_i^*|, \tag{21}$$

where $\breve{F}_i$ is the cumulative distribution function of the ith margin of the probabilistic forecast, $\breve{Y}_i$ and $\breve{Y}_i^*$ are independent copies of a random variable with distribution $\breve{F}_i$, and y_i is the outcome of the ith margin. The expectations in the second line can be approximated by Monte Carlo when a sample from the predictive distribution is available.

An advantage to this approach is that it allows the forecaster to evaluate the levels and individual series of the hierarchy where the gains from reconciliation are greatest. For this reason this approach has been used in the limited literature on probabilistic forecasting for hierarchies (Ben Taieb et al. 2017, Jeon et al. 2018) to date. A major shortcoming of this approach however, is that evaluating univariate scores on the margins does not account for the dependence in the hierarchy.

4.2 Multivariate scoring rules

While a number of alternative proper scoring rules are available for univariate forecasts, the multivariate case is somewhat more limited. Here we focus on three scoring rules: the log score, the energy score and the variogram score.

The log score can be approximated using a sample of values from the probabilistic forecast density (Jordan et al. 2017); however it is more commonly used when a parametric form for the density is available for the probabilistic forecast.

The energy score on the other hand can be defined in terms of the characteristic function of the probabilistic forecast, but the representation in terms of expectations leads itself to

easy computation when samples from the probabilistic forecast are available. An interesting limiting case is where $\alpha = 2$, where it can be easily shown that energy score simplifies to mean squared error around the mean of the predictive distribution. In this limiting case, the energy score is proper but not strictly proper. Pinson & Tastu (2013) also argue that the energy score has low discriminative ability for incorrectly specified covariances, even though it discriminates the misspecified means well.

In contrast, Scheuerer & Hamill (2015) have shown that the variogram score has a higher discrimination ability for misspecified means, variances and correlation structures than the energy score. When $\breve{\boldsymbol{y}}$ is a random variable from probabilistic forecast $\breve{F}$, the empirical variogram score is defined as

$$\mathrm{VS}(\breve{F}, \boldsymbol{y}) = \sum_{i=1}^{n} \sum_{j=1}^{n} w_{ij} \left(|y_i - y_j|^p - E_{\breve{Y}_i, \breve{Y}_j} |\breve{Y}_i - \breve{Y}_j|^p \right)^2. \tag{22}$$

Scheuerer & Hamill (2015) recommend using $p = 0.5$.

4.2.1 Comparing unreconciled forecasts to reconciled forecasts

For both reconciled and unreconciled densities it is possible to obtain a density from the probability measures defined in Section 2. Therefore it may seem sensible to compare unreconciled densities to reconciled densities on the basis of log score. However, the following theorem shows that using the log score may fail in the case of multivariate distributions with a degeneracy.

Theorem 4.1 (Impropriety of log score). *When the true data generating process is coherent, then the log score is improper with respect to the class of incoherent measures.*

Proof. Consider a rotated version of hierarchical time series, $\boldsymbol{z}_t = \boldsymbol{U}\boldsymbol{y}_t$, so that the first m elements of $\boldsymbol{z}_t$ denoted $\boldsymbol{z}_t^{(1)}$ are unconstrained, while the remaining $n - m$ elements denoted

24

$z_t^{(2)}$ equal 0 when the aggregation constraints hold. An example of the $n \times n$ $\boldsymbol{U}$ is the matrix of left singular vectors of $\boldsymbol{S}$.

Consider the case where the true predictive density is $f_1(z_t^{(1)})\mathbb{1}\left(z_t^{(2)} = \boldsymbol{0}\right)$, and we evaluate an incoherent density given by $f_1(z_t^{(1)})f_2(z_t^{(2)})$, where f_2 is highly concentrated around 0 but still non-degenerate. For example, f_2 may be Gaussian with variance $\sigma^2 \boldsymbol{I}$ with $\sigma^2 < (2\pi)^{-1}$. The log score under the true data generating process is

$$S\left(f, z_t^{(1)}\right) = -\log f_1\left(z_t^{(1)}\right),$$

while that of the unreconciled density is

$$S\left(\hat{f}, z_t^{(1)}\right) = -\log f_1(z_t^{(1)}) - f_2(z_t^{(1)}) \tag{23}$$

$$= -\log f_1(z_t^{(1)}) + \frac{n-m}{2}\log(2\pi\sigma^2) \tag{24}$$

$$< -\log f_1(z_t^{(1)}) = S\left(f, z_t^{(1)}\right). \tag{25}$$

After taking expectations $ES(f, f) > ES(\hat{f}, f)$, violating the condition in Equation (19) for a proper scoring rule. $\qquad\square$

A similar issue also arises when discrete random variables are modelled as if they were continuous, an issue discussed in Section 4.1 of Gneiting & Raftery (2007). This implies that the log score should be avoided when comparing reconciled and unreconciled probabilistic forecasts.

4.2.2 Comparing reconciled forecasts to one another

Coherent probabilistic forecasts can be completely characterised in terms of basis series; if a probabilistic forecast is available for the basis series, then a probabilistic forecast can be recovered for the entire hierarchy via Definition 2.3. This may suggest that it is adequate

to merely compare two coherent forecasts to one another using the basis series only. We now show how this depends on the specific scoring rule used.

For the log score, suppose the coherent probabilistic forecast has density $f(\boldsymbol{b})$. The density for the full hierarchy is given by $f(\boldsymbol{y}) = f(\boldsymbol{Sb}) = f(\boldsymbol{b})J^{-1}$, where $J = \prod_{j=1}^{m} \lambda_j$ is a pseudo-determinant of the non-square matrix $\boldsymbol{S}$ and λ_j are the non-zero singular values of $\boldsymbol{S}$. Therefore for any coherent density, the log score of the full hierarchy differs from the log score for the bottom-level series by the term $log(J)$. This term depends only on the structure of the hierarchy and is fixed across different reconciliation methods. Therefore if one method achieves a lower expected log score compared to an alternative method using the bottom-level series only, the same ordering is preserved when an assessment is made on the basis of the full hierarchy.

The same property does not hold for all scores in general. For example, the energy score can be expressed in terms of expectations of norms. In general, since norms are invariant under orthogonal rotations, the energy score is also invariant under orthogonal transformations (Székely & Rizzo 2013, Gneiting & Raftery 2007). In the context of two coherent forecasts, the same is true of a semi-orthogonal transformation from a lower dimensional basis series to the full hierarchy. However, when $\boldsymbol{S}$ is the usual summing matrix, it is not semi-orthogonal. Therefore the energy score computed on the bottom-level series will differ from the energy score computed using the full hierarchy and the ordering of different reconciliation methods may change depending on the basis series used. In this case we recommend computing the energy score using the full hierarchy. Although the discussion here is related to energy score, the same logic holds for other multivariate scores, for example the variogram score.

The properties of multivariate scoring rules in the context of evaluating reconciled probabilistic forecasts are summarised in Table 2.

26

	Coherent v Incoherent	Coherent v Coherent
Log Score	Not proper	Ordering preserved if compared using bottom-level only
Energy/ Variogram Score	Proper	Full hierarchy should be used

Table 2: Summary of properties of scoring rules in the context of reconciled probabilistic forecasts.

5   Simulation study

We now turn our attention to comparing different reconciliation methods in a simulation study where the data is conditionally Gaussian. We choose the Gaussian case due to its analytical tractability which allows for evaluation using all scoring rules (including the log score). The non-Gaussian case lies beyond the scope of this simulation study.

For the data generating process, we consider the hierarchy given in Figure 1, comprising two aggregation levels with four bottom-level series. Each bottom-level series will be generated first, and then summed to obtain the data for the upper-level series. In practice, hierarchical time series tend to contain much noisier series at lower levels of aggregation. In order to replicate this feature in our simulations, we follow the data generating process proposed by Wickramasuriya et al. (2018).

First $\{w_{AA,t}, w_{AB,t}, w_{BA,t}, w_{BB,t}\}$ are generated from ARIMA(p, d, q) processes, where (p, q) and d take integers from $\{1, 2\}$ and $\{0, 1\}$ respectively with equal probability. The errors driving these ARIMA processes are jointly normal, and denoted by $\{\varepsilon_{AA,t}, \varepsilon_{AB,t}, \varepsilon_{BA,t}, \varepsilon_{BB,t}\} \overset{iid}{\sim} \mathcal{N}(\mathbf{0}, \boldsymbol{\Sigma}) \; \forall t$. The parameters for the AR and MA components are randomly and uniformly generated from $[0.3, 0.5]$ and $[0.3, 0.7]$ respectively. Then the bottom-level series

$\{y_{AA,t}, y_{AB,t}, y_{BA,t}, y_{BB,t}\}$ are given by:

$$y_{AA,t} = w_{AA,t} + u_t - 0.5v_t,$$

$$y_{AB,t} = w_{AB,t} - u_t - 0.5v_t,$$

$$y_{BA,t} = w_{BA,t} + u_t + 0.5v_t,$$

$$y_{BB,t} = w_{BB,t} - u_t + 0.5v_t,$$

where $u_t \sim \mathcal{N}(0, \sigma_u^2)$ and $v_t \sim \mathcal{N}(0, \sigma_v^2)$. The aggregate series in the middle-level are given by:

$$y_{A,t} = w_{AA,t} + w_{AB,t} - v_t,$$

$$y_{B,t} = w_{BA,t} + w_{BB,t} + v_t,$$

and the total series is given by

$$y_{Tot,t} = w_{AA,t} + w_{AB,t} + w_{BA,t} + w_{BB,t}.$$

To ensure the disaggregate series are noisier than the aggregate series, we choose $\boldsymbol{\Sigma}, \sigma_u^2$ and σ_v^2 such that

$$\mathrm{Var}(\varepsilon_{AA,t} + \varepsilon_{AB,t} + \varepsilon_{BA,t} + \varepsilon_{BB,t}) \leq \mathrm{Var}(\varepsilon_{AA,t} + \varepsilon_{AB,t} - v_t) \leq \mathrm{Var}(\varepsilon_{AA,t} + u_t - 0.5v_t),$$

and similar inequalities hold when $\varepsilon_{AA,t}$ is replaced by $\varepsilon_{AB,t}$, $\varepsilon_{BA,t}$ and $\varepsilon_{BB,t}$ in the third term. The values of $\boldsymbol{\Sigma}$, σ_u^2 and σ_v^2 that we use and which satisfy these constraints are $\sigma_u^2 = 19$, $\sigma_u^2 = 18$ and

$$\boldsymbol{\Sigma} = \begin{pmatrix} 5.0 & 3.1 & 0.6 & 0.4 \\ 3.1 & 4.0 & 0.9 & 1.4 \\ 0.6 & 0.9 & 2.0 & 1.8 \\ 0.4 & 1.4 & 1.8 & 3.0 \end{pmatrix}.$$

We generate data with a sample size of $T = 501$. Univariate ARIMA models are selected for each series using the *auto.arima* function in the *forecast* package (Hyndman 2017) in R (R Core Team 2018). The same package was used to fit each series independently using the first 500 observations, and evaluate 1-step ahead base (incoherent) probabilistic forecasts. These were then reconciled using different projections summarised in Table 1. This process was replicated using 1000 different data sets from the same data generating processes.

To assess the predictive performance of different forecasting methods, we use scoring rules as discussed in Section 4. To facilitate comparisons, we report skill scores (Gneiting & Raftery 2007). For a given forecasting method, evaluated by a particular scoring rule, the skill score gives the percentage improvement of the preferred forecasting method relative to a reference method. A negative valued skill score indicates that a method is worse than the reference method, whereas any positive value indicates that method is superior to the reference method.

Table 3 summarizes the forecasting performance of unreconciled, bottom-up, OLS, WLS and two MinT reconciliation methods using log score, energy score and variogram score. In all cases skill scores are calculated with the bottom-up method as reference. All log scores are evaluated on the basis of bottom-level series only, however these only differ from the log scores for the full hierarchy by a fixed constant. The cell for log score of unreconciled forecasts is left blank since the log score is not proper in this context. Overall, the MinT methods provide the best performance irrespective of the scoring rule, and all methods that reconcile using information at all levels of the forecast improve upon unreconciled forecasts. Bottom-up forecasts perform even worse than unreconciled forecasts in some cases.

Tables 4 and 5 break down the forecasting performance of different reconciliation methods by considering univariate scores on each individual margin. Tables 4 summarises results for the top and middle-level, Table 5 does the same for bottom-level. The log score and

Table 3: Comparison of coherent forecasts. "Energy score" and "Variogram score" columns give scores based on the joint forecast distribution of the whole hierarchy. "Log score" column gives the log scores of the joint forecast distribution of the bottom-level. "Skill score" columns give the percentage skill score with reference to the bottom-up method. Entries in these columns show the percentage increase of scores for different reconciliation methods relative to the bottom-up method.

Forecasting method	Energy score		Variogram score		Log score	
	Mean score	Skill score %	Mean score	Skill score %	Mean score	Skill score %
MinT(Shrink)	10.03	18.79	8.44	8.46	11.30	6.22
MinT(Sample)	10.01	18.95	8.41	8.79	11.29	6.31
MinT(WLS)	10.53	14.74	9.02	2.17	12.61	−4.65
OLS	10.53	14.74	8.86	3.09	11.54	4.23
Bottom-up	12.35		9.22		12.05	
Incoherent	11.12		9.53			

CRPS are considered, while skill scores are computed with the unreconciled forecast as a reference. When broken down in this fashion, the methods based on MinT perform best for all series and always outperform bottom-up and unreconciled forecasts.

6   Conclusions

By redefining coherent forecasts and forecast reconciliation in geometric terms, we have established two new theoretical results that support the use of projections for point forecast reconciliation, and have allowed us to extend these concepts to probabilistic forecasting. We have shown that for elliptical distributions the true predictive density can be recovered

Table 4: Comparison of incoherent vs coherent forecasts based on the univariate forecast distribution of aggregate series. The "Incoherent" row shows the average scores for incoherent forecasts. Each entry above this row represents the percentage skill score with reference to the incoherent forecasts. These entries show the percentage increase in score for different forecasting methods relative to the incoherent forecasts.

Forecasting	Total		Series - A		Series - B	
method	CRPS	LogS	CRPS	LogS	CRPS	LogS
MinT(Shrink)	0.74	0.00	10.49	3.24	9.16	2.73
MinT(Sample)	0.74	0.00	10.49	3.24	9.16	2.73
MinT(WLS)	−2.96	−2.36	6.10	−4.12	5.66	−3.03
OLS	−9.26	−3.36	7.07	2.06	7.01	1.82
Bottom-up	−91.48	−22.22	−8.05	−2.06	−6.20	−1.82
Incoherent	*2.70*	*2.97*	*4.10*	*3.40*	*3.71*	*3.30*

Table 5: Comparison of incoherent vs coherent forecasts based univariate forecast distribution of bottom-level series. The "Incoherent" row shows the average scores for incoherent forecasts.

Forecasting	Series - AA		Series - AB		Series - BA		Series - BB	
method	CRPS	LogS	CRPS	LogS	CRPS	LogS	CRPS	LogS
MinT(Shrink)	7.61	2.43	10.82	3.02	5.93	1.86	7.76	2.47
MinT(Sample)	7.88	2.43	11.08	3.02	6.20	1.86	8.05	2.47
MinT(WLS)	3.53	0.00	6.33	0.60	2.43	−0.62	4.89	0.62
OLS	2.99	0.91	5.28	1.51	2.90	0.62	4.31	1.23
Incoherent	*3.68*	*3.29*	*3.79*	*3.31*	*3.45*	*3.22*	*3.48*	*3.24*

by linear reconciliation and we have established conditions for when this is a projection. Although this projection cannot feasibly be obtained in practice, a projection similar to the MinT procedure provides a good approximation in applications. This is supported by the results of a simulation study. Finally, we have also discussed strategies for evaluating probabilistic forecasts for hierarchical time series advocating the use of multivariate scoring rules on the full hierarchy, while establishing a key result regarding the impropriety of the log score with respect to incoherent forecasts.

In many ways this paper sets up a substantial future research agenda. For example, having defined what amounts to an entire class of reconciliation methods for probabilistic forecasts it will be worthwhile investigating which specific projections are optimal. This is likely to depend on the specific scoring rule employed as well as the properties of the base forecasts. Another avenue worth investigating is to consider whether it is possible to recover the true predictive distribution for non-elliptical distributions via a non-linear function $g(.)$.

References

Athanasopoulos, G., Ahmed, R. A. & Hyndman, R. J. (2009), 'Hierarchical forecasts for australian domestic tourism', *International Journal of Forecasting* **25**(1), 146 – 166.
  URL: *http://www.sciencedirect.com/science/article/pii/S0169207008000691*

Athanasopoulos, G., Hyndman, R. J., Kourentzes, N. & Petropoulos, F. (2017), 'Forecasting with temporal hierarchies', *European Journal of Operational Research* **262**(1), 60–74.

Ben Taieb, S., Huser, R., Hyndman, R. J. & Genton, M. G. (2017), 'Forecasting uncertainty in electricity smart meter data by boosting additive quantile regression', *IEEE Transactions on Smart Grid* **7**(5), 2448–2455.

Dunn, D. M., Williams, W. H. & Dechaine, T. L. (1976), 'Aggregate Versus Subaggregate Models in Local Area Forecasting', *Journal of American Statistical Association* **71**(353), 68–71.

Gneiting, T. & Katzfuss, M. (2014), 'Probabilistic Forecasting', *Annual Review of Statistics and Its Application* **1**, 125–151.

Gneiting, T. & Raftery, A. E. (2007), 'Strictly Proper Scoring Rules, Prediction, and Estimation', *Journal of the American Statistical Association* **102**(477), 359–378.

Gneiting, T., Stanberry, L. I., Grimit, E. P., Held, L. & Johnson, N. A. (2008), Assessing probabilistic forecasts of multivariate quantities, with an application to ensemble predictions of surface winds.

Gross, C. W. & Sohl, J. E. (1990), 'Disaggregation methods to expedite product line forecasting', *Journal of Forecasting* **9**(3), 233–254.

Hunter, J. K. & Nachtergaele, B. (2001), *Applied analysis*, World Scientific Publishing Company.

Hyndman, R. (2017), 'forecast: Forecasting Functions for Time Series and Linear Models, R package version 8.0', *URL: http://github.com/robjhyndman/forecast* .

Hyndman, R. J., Ahmed, R. A., Athanasopoulos, G. & Shang, H. L. (2011), 'Optimal combination forecasts for hierarchical time series', *Computational Statistics and Data Analysis* **55**(9), 2579–2589.

Hyndman, R. J. & Athanasopoulos, G. (2018), *Forecasting: principles and practice, 2nd Edition*, OTexts.

Jeon, J., Panagiotelis, A. & Petropoulos, F. (2018), 'Reconciliation of probabilistic forecasts with an application to wind power'. Working Paper.

Jordan, A., Krüger, F. & Lerch, S. (2017), 'Evaluating probabilistic forecasts with the R package scoringRules'.
URL: *http://arxiv.org/abs/1709.04743*

Pinson, P. & Tastu, J. (2013), Discrimination ability of the Energy score, Technical report, Technical University of Denmark.

R Core Team (2018), *R: A Language and Environment for Statistical Computing*, R Foundation for Statistical Computing, Vienna, Austria.
URL: *https://www.R-project.org/*

Schäfer, J. & Strimmer, K. (2005), 'A Shrinkage Approach to Large-Scale Covariance Matrix Estimation and Implications for Functional Genomics', *Statistical Applications*

in Genetics and Molecular Biology **4**(1).

URL: *https://www.degruyter.com/view/j/sagmb.2005.4.issue-1/sagmb.2005.4.1.1175/sagmb.2005.4.1.1175.xml*

Scheuerer, M. & Hamill, T. M. (2015), 'Variogram-Based Proper Scoring Rules for Probabilistic Forecasts of Multivariate Quantities', *Monthly Weather Review* **143**(4), 1321–1334.

Székely, G. J. & Rizzo, M. L. (2013), 'Energy statistics: A class of statistics based on distances', *Journal of Statistical Planning and Inference* **143**(8), 1249–1272.
URL: *http://dx.doi.org/10.1016/j.jspi.2013.03.018*

van Erven, T. & Cugliari, J. (2014), *Game-Theoretically Optimal reconciliation of contemporaneous hierarchical time series forecasts.*

Wickramasuriya, S. L., Athanasopoulos, G. & Hyndman, R. J. (2018), 'Optimal forecast reconciliation for hierarchical and grouped time series through trace minimization', *J American Statistical Association* . to appear.